Addressable Nanowell Arrays Formed Using Reversibly Sealable Hybrid Elastomer–Metal Stencils

ARTICLE *in* ANALYTICAL CHEMISTRY · APRIL 2010

Impact Factor: 5.64 · DOI: 10.1021/ac100335d · Source: PubMed

Anal. Chem. **XXXX,** *xxx,* 000–000

Addressable Nanowell Arrays Formed Using Reversibly Sealable Hybrid Elastomer-Metal Stencils

Mateu Pla-Roca,[†] Rym Feriel Leulmi,[†] Haig Djambazian,[‡] Saravanan Sundararajan,[§] and David Juncker*[,†,‡,||]

Biomedical Engineering Department, McGill University, and McGill University and Genome Quebec Innovation Centre, 740 Dr. Penfield Drive, Montreal, Quebec, Canada H3A 1A4, Department of Human Genetics, McGill University, 1205 Dr. Penfield Drive Montreal, Quebec, Canada H3A 1B1, and Department of Neurology and Neurosurgery, McGill University, 740 Dr. Penfield Drive, Montreal, Quebec, Canada H3A 1A4

There are two major array formats used in life science research and biomedical analysis. The first is the microwell plate format with millimeter-sized wells each with microliter capacity addressed individually and repeatedly during experiments. The second is the microarray format with micrometer-sized spots that are patterned initially but not addressable individually thereafter. Here, we present an addressable nanoliter-well plate with micrometer sized wells that combines the advantages of the two array formats. The nanowells are formed by reversibly sealing a steel stencil featuring an array of micrometer-scale openings to an optically transparent substrate. The nanowells have a capacity of ~1 nL, are ~140 μm in diameter, and are arrayed at a density of 1600 wells cm^{-2}. A soft polymer is patterned photolithographically around each opening so as to form a microgasket for pressure sensitive, liquid tight, and reversible sealing to any type of smooth substrate, either hydrophilic or hydrophobic. The rigidity of the steel prevents the distortion that occurs in soft, all-polymeric stencils and permits accurate registration across the entire array, which in turn allows for repeated, individual addressing of wells using an inkjet spotter. The stencils are used to pattern cells, make protein microarrays, and create nanowells on surfaces to study reverse transfection by first spotting plasmids encoding fluorescent proteins into the wells, seeding cells, and monitoring the transfection of the cells in real time using time-lapse imaging. The hybrid elastomer-metal stencils (HEMSs) are versatile and useful for multiplexed analysis of drugs, biomolecules, and cells with microarray density.

Microwell or multititer plates (MTP) have long been used in analytical research and diagnostic settings to perform multiple assays with biomolecules or cells in parallel. Despite a progressive reduction in the size of the well (and thus an increase of the well's density), the volume required still remains in the microliter range and only 4 assays per mm^2 can be carried out on high-density plates with 3456 wells and 2.6 μL capacity per well. Further miniaturization of MTP toward wells with nanoliter capacity, or nanowell plates, would be advantageous as it allows a much larger number of assays to be done while saving precious reagents and analytes (i.e., antibodies, purified proteins, DNA, patient samples). In addition, the use of nanowells may allow more rapid data acquisition because multiple wells can fit into the field of view of a microscope, which is needed for imaging when performing miniaturized cells assays.

A challenge to implementing biological assays using nanowell plates is the interfacing and alignment with a liquid handling robot that is required for robust and high-throughput addressing of solutions to each nanowell. The XY coordinates of the wells can readily be computed; however, a small deviation in the center-to-center distance between wells (for example, due to shrinkage, skewing, or strain) added over thousands of wells will inevitably lead to mismatch between the calculated and actual positions of the wells. Using microfabrication techniques and etching, rigid materials such as silicon (Si) or glass can be patterned with arrays of precisely aligned wells.[1−4] However, such arrays are brittle and opaque when silicon is used, and glass is difficult and expensive to micromachine because dry etching processes are inefficient, while wet etching is slow. Hybrid Si and glass microwell arrays have also been fabricated by irreversibly bonding a silicon stencil onto a glass slide[5] in order to combine the better etching efficiency of the silicon and the transparency of glass but with relatively large 500 nL microwells and a density of ~44 wells cm^{-2}.

* To whom correspondence should be addressed. E-mail: david.juncker@mcgill.ca.

[†] Biomedical Engineering Department, McGill University.

[‡] McGill University and Genome Quebec Innovation Centre.

[§] Department of Human Genetics, McGill University.

[||] Department of Neurology and Neurosurgery, McGill University.

(1) Young, I. T.; Moerman, R.; Doel, L. R. V. D.; Iordanov, V.; Kroon, A.; Dietrich, H. R. C.; Dedem, G.; Bossche, A.; Gray, B. L.; Sarro, L.; Verbeek, P. W.; Vliet, L. J. V. *J. Microsc.* **2003**, *212*, 254–263.

(2) Moerman, R.; Knoll, J.; Apetrei, C.; van den Doel, L. R.; van Dedem, G. W. K. *Anal. Chem.* **2004**, *77*, 225–231.

(3) Angenendt, P.; Nyarsik, L.; Szaflarski, W.; Glokler, J.; Nierhaus, K. H.; Lehrach, H.; Cahill, D. J.; Lueking, A. *Anal. Chem.* **2004**, *76*, 1844–1849.

(4) Molter, T. W.; McQuaide, S. C.; Suchorolski, M. T.; Strovas, T. J.; Burgess, L. W.; Meldrum, D. R.; Lidstrom, M. E. *Sens. Actuators, B* **2009**, *135*, 678–686.

(5) Lindström, S.; Larsson, R.; Svahn, H. A. *Electrophoresis* **2008**, *29*, 1219–1227.

10.1021/ac100335d

Polymeric nanowells on the other hand can be made, for example, by laser ablation of poly(methylmethacrylate) (PMMA),[6] hot embossing into polystyrene,[7] or injection-molding of acrylonitrile butadiene styrene (ABS).[8] The initial costs for setting up an injection-molding facility are, however, very high, and polymer plates suffer from residual fluorescence, are restricted when it comes to tuning the surface chemistry, and can only tolerate a limited range of solvents. Finally, in all above cases, automated, high-throughput robotized addressing of the nanowells has not been demonstrated.

An alternative strategy to create nanoplates uses microstencils that spontaneously seal to a flat surface, thereby forming liquid-tight nanowells. This configuration enables flexibility in choosing the substrate and allows functionalizing its surface independently before assembly with the stencil. Moreover, if glass coverslips are used as substrates, high resolution phase contrast and fluorescence microscopy can be used for imaging objects through the substrate.

Microstencils made of soft silicones such as polydimethylsiloxane (PDMS) have been used to pattern biomolecules or cells on surfaces.[9−11] The softness and elasticity of PDMS leads to spontaneous sealing to any smooth surface by forming a so-called conformal contact, which greatly facilitates the fabrication of nanowell arrays. The downside is that the elasticity of PDMS and the shrinkage that occurs during fabrication lead to distortion and irregular arrays which cannot be aligned to a regular matrix of positions, precluding automated addressing. Recently, Parylene-C stencils have been proposed as reversibly sealable stencils for use in protein and cell patterning. Parylene-C stencils are, unlike PDMS stencils, reusable, free-standing, and rigid, creating regularly arranged nanowells when sealed.[12−14] However, Parylene-C does not form a conformal contact, and the liquid confinement is, thus, dependent on the hydrophobicity of both the substrate surface and the stencil, which limits its application to hydrophobic surfaces,[15,16] for instance preventing the use of clean glass as a substrate.

Here, we introduce reversibly sealable, rigid stencils used for forming regular nanowell arrays on transparent, hydrophobic, and hydrophilic substrates. They are named nanowells because their volume is nanoliters and their dimension is micrometers, which mirrors microwell plates that accommodate microliter volumes but several millimeters wide. The nanowell arrays are made up of a steel stencil with an array of openings, each of which is surrounded by a soft elastomeric ring. Such hybrid elastomer-metal stencils (HEMSs) benefit from the outstanding mechanical characteristics of steel sheets with high rigidity, toughness, and flexibility and from the spontaneous sealing properties of soft elastomers that form a conformal contact with smooth surfaces. The hybrid assembly, thus, allows reversibly sealing the stencils to both hydrophilic and hydrophobic surfaces, reusing them, all while maintaining a high positional accuracy of each well for robotic addressing. We describe the microfabrication of HEMS, their characterization, and their application to proteomics and cell biology.

EXPERIMENTAL SECTION

UV Curable Polymers and Chemicals. UV curable elastomers Semicosil 964 UV and Semicosil 936 were acquired from Wacker Chemical Corporation (Adrian, MI); Dymax-103, Dymax-105, and Dymax-107 were obtained from Dymax Corporation (Torrington, CT). Upon reception, the photopolymers were stored at 4 °C and protected from light. 3-(Trimethoxysilyl)propyl methacrylate (TMSMA) was purchased from Sigma-Aldrich (Oakville, ON) and stored at 0 °C. Isopropanol (IPA), methylethylketone (MEK), chloroform, dicholoromethane (DCM), xylene, and toluene were obtained from Fisher Scientific (Pittsburgh, PA).

Steel Stencils and Photolithographic Masks. The steel stencils (Sefar Printing Solutions, Arden Hills, MN) and photomask (Fineline Imaging, Colorado Springs, CO) were designed in house using mask design software (Clewin 4.3, Wieweb, Hengelo, Netherlands). Each steel stencil (50 μm thick) contains 2592 rounded microapertures, 120−150 μm in diameter, arranged as 32 subarrays (4×8) of 81 microapertures (9×9). The subarrays are themselves arrayed with a 4.5 mm pitch compatible with the American National Standards Institute (ANSI) standard. The center to center distance of the openings is 250 μm (i.e., 1600 openings per cm^2). The microgaskets were designed as 35 μm wide rings (Figure S-1 in the Supporting Information). The steel stencils and the photomask feature alignment marks for registration during the fabrication process (Figure S-2 in the Supporting Information). Each photomask contains three exact designs of microgasket arrays allowing the patterning of microgaskets on up to three steel stencils simultaneously. Steel stencils contain tabs that connect them during the fabrication process (Figure S-3 in the Supporting Information).

Functionalization of the Steel Stencils. The steel stencils were treated with an air plasma (TEGAL 415, Plasmaline), soaked in 1% 3-(Trimethoxysilyl)propyl methacrylate (TMSMA) in toluene during 20 min, and rinsed with toluene. The stencils were oven-baked during 10 min at 110 °C in order to ensure a complete reaction between the silane and the steel surface.

HEMS Microfabrication. The sealable HEMS were fabricated in batches of three. Dymax-103 polymer was diluted in toluene (2:1) and was spin coated on coverslips (Fisher, 20 mm × 40 mm, number 1.5) for 10 s at 500 rpm followed by 30 s at 2000 rpm. Samples were then baked on a hot plate for 5 min at 70 °C in order to evaporate the toluene. Using tweezers, the coverslips were placed over the steel stencils and gently pressed. The sandwich assembly was then placed in the mask aligner (EVG Aligner, Albany, NY), and the steel openings and microgasket designs were aligned using the alignment marks. The coverslip protects the photomask from the tacky photopolymer during

(6) Becker, H.; Gärtner, C. *Rev. Mol. Biotechnol.* **2001**, *82*, 89–99.
(7) Dusseiller, M. R.; Schlaepfer, D.; Koch, M.; Kroschewski, R.; Textor, M. *Biomaterials* **2005**, *26*, 5917–5925.
(8) Seidel, M.; Gauglitz, G. *Trends Anal. Chem.* **2003**, *22*, 385–394.
(9) Ostuni, E.; Kane, R.; Chen, C. S.; Ingber, D. E.; Whitesides, G. M. *Langmuir* **2000**, *16*, 7811–7819.
(10) Folch, A.; Jo, B.-H.; Hurtado, O.; Beebe, D. J.; Toner, M. *J. Biomed. Mater. Res.* **2000**, *52*, 346–353.
(11) Khetani, S. R.; Bhatia, S. N. *Nat. Biotechnol.* **2008**, *26*, 120–126.
(12) Tan, C. P.; Seo, B. R.; Brooks, D. J.; Chandler, E. M.; Craighead, H. G.; Fischbach, C. *Integr. Biol.* **2009**, *1*, 587–594.
(13) Wright, D.; Rajalingam, B.; Selvarasah, S.; Dokmeci, M. R.; Khademhosseini, A. *Lab Chip* **2007**, *7*, 1272–1279.
(14) Wright, D.; Rajalingam, B.; Karp, J. M.; Selvarasah, S.; Ling, Y.; Yeh, J.; Langer, R.; Dokmeci, M. R.; Khademhosseini, A. *J. Biomed. Mater. Res., Part A* **2008**, *85A*, 530–538.
(15) Juncker, D.; Schmid, H.; Bernard, A.; Caelen, I.; Michel, B.; Rooij, N.d.; Delamarche, E. *J. Micromech. Microeng.* **2001**, *11*, 532–541.
(16) Delamarche, E.; Juncker, D.; Schmid, H. *Adv. Mater.* **2005**, *17*, 2911–2933.

the alignment process. After flood exposure during 30 s (11.5 mW/cm^2), the coverslips were peeled off carefully and the stencils were developed for 10 s in toluene. Finally, the HEMSs were dried under a flow of nitrogen and cut apart. The yield of the fabrication process for HEMS is above 80%, and the fabrication defects identified could all be attributed to dust particles that are contained in the prepolymer solution. Before cell culture experiments, the HEMSs were immersed in methyethylketone (1 h) and ethanol (1 h) before being dried under a flow of nitrogen. This process was performed to remove the presence of dust particles and to extract un-cross-linked monomers from the microgaskets in order to improve biocompatibility.

Characterization of HEMS. The quality of the fabricated HEMS was verified by optical microscopy (LV150 industrial microscope, Nikon, Japan). Scanning electron microscopy (SEM) images (Hitachi S-3000N Variable Pressure) were obtained using HEMS coated with a 5 nm gold/palladium alloy and used to measure the width and thickness of the gaskets.

Sealing Studies on Hydrophilic and Hydrophobic Surfaces. The sealing of the HEMS was tested on untreated and epoxy-coated microscope slides (Schott AG, Elmsford, NY), polystyrene cell culture plates (100 × 20 mm, Corning, Lowell, MA), polystyrene cell culture plates hydrophilized with an air plasma, and poly-L-lysine (PLL) (Sigma-Aldrich) coated microscope slides. PLL coating was performed by incubation of 1 mg/mL poly-L-lysine solution in PBS (10 mM adjusted to pH 7.4) on a microscope slide previously activated in a 2 M NaOH solution in 75% ethanol during 30 min.

HEMS Based Cell Patterning. The HEMSs were sterilized under UV light in a biological safety cabinet for 10 min and sealed immediately on cell culture dishes (100 × 20 mm, Corning, Lowell, MA). Fifteen milliliters of DMEM cell culture media (Dulbecco's Modified Eagle Medium, Invitrogen, Burlington, ON) was added and the dish was centrifuged at 2000 rpm for 10 min to remove air bubbles trapped within the nanowells (Figure S-4 in the Supporting Information). Five milliliters of media containing 20 000 C2C12 cells/mL was then added. The cells were allowed to settle for 1 h, after which the media was changed twice to rinse away cells lying outside the nanowells. After 1 h of incubation, the HEMSs were peeled off with the help of sharp tweezers. The cells patterned on the surface were imaged with differential interference contrast light microscopy (TE-2000E inverted microscope, Nikon, Japan).

Inkjet Delivery of Solutions. An inkjet microarrayer equipped with an optical target recognition system (Nanoplotter NP 2.0, Gesim, Groserkmannsdorf, Germany) (ac10033d_si_002.avi in the Supporting Information) was used to dispense solutions in individual nanowells. Spotting was performed in 75% humidity on substrates cooled to 16 °C in order to prevent evaporation of the solution. Static charges on the stencils were removed with an antistatic gun (Antistatic gun, Mettler-Toledo, Columbus, OH) prior to being addressed with the inkjet spotter. Each drop dispensed by the inkjet is approximately 0.4 nL. In order to ensure the complete filling of the nanowells, 1.2 nL (3 drops) was dispensed.

Protein Printing. The HEMSs were sealed on epoxy-coated microscope slides and addressed with 100 μg/mL Chicken antigoat IgG (Invitrogen) labeled with green fluorescence dye (AF488) and 100 μg/mL streptavidin labeled with red fluorescence dye (AF548) in PBS containing 5% glycerol. Proteins were then incubated for 1 h on the microarrayer tray. Imaging of the printed slides was performed using a laser scanner (LSReloaded, Tecan, Männedorf, Switzerland).

DNA Printing. Expression vectors for green fluorescent protein (EGFP) and cyan fluorescent protein (ECFP) expression controlled by the CMV immediate early promoter-enhancer (Clontech, Mountain View, CA) were prepared using Qiagen DNA Purification Kits (Qiagen, Mississauga, ON). For spotting, 15 μL of a solution containing each expression vector (final concentration 33 ng DNA/μL) was prepared by mixing 500 ng of plasmid DNA, 0.5 μL of Lipofectamine 2000 (Invitrogen), 11.5 μL of Optimem culture medium (Invitrogen), and 3 μL of 0.1% fibronectin (Sigma-Aldrich), prepared as a solution in PBS. Before printing, the HEMSs were sterilized under UV light in a biological safety cabinet for 10 min and sealed immediately on cell culture dishes (100 × 20 mm, Corning). Once the printing was completed, the samples where dried in a vacuum desiccator for 1 h. Fifteen milliliters of antibiotic free DMEM cell culture media was poured over the HEMS and then centrifuged at 2000 rpm for 10 min in order to remove air bubbles trapped in the nanowells. Immediately after, 5 mL of media containing HEK 293T human epithelial kidney cells at a density of 40 000 cells/mL was added, and the cells were allowed to settle for 1 h. The media was then changed twice in order to remove the cells that were not deposited within the nanowells. After 24 h of incubation at 5% CO_2 and 37 °C, the cells started to express the corresponding GFP and CFP proteins in individual nanowells. Time-lapse imaging of the GFP- and CFP-expressing cells was performed in phenol-red free DMEM media (Invitrogen) supplemented with antibiotics using an epifluorescence inverted microscope (TE-2000E, Nikon, Japan) equipped with specific excitation (488 and 433 nm, respectively) and emission (507 and 475 nm, respectively) filters. Acquisition of distinct nanowells was performed automatically using the microscope's motorized stage.

RESULTS AND DISCUSSION

The HEMSs are based on a steel stencil that acts as a rigid support and on microgaskets made of a soft elastomeric polymer which upon contact with a flat surface forms a liquid-tight seal, creating an array of nanowells (Figure 1). Solutions dispensed into the nanowells are confined to a small area on the surface. At any time, the HEMS can be detached from the surface while leaving a microarray of spots.

The microgaskets are produced by photopatterning of a UV sensitive, photocurable elastomer on the steel stencils. Several different types of photocurable elastomers have been reported. (Methacryloxypropyl)methylsiloxane-dimethylsiloxane (sold as RMS-033) and PDMS polymers can be turned into negative resists after the addition of photoinitiators; however, they are sensitive to inhibition by oxygen.[17−19] Alternatively, regular PDMS can be mixed with benzophenone which inhibits the curing agent and polymerization following UV exposure, thus transforming PDMS

(17) Torbiéro, B.; Pourciel-Gouzy, M. L.; Humenyuk, I.; Doucet, J. B.; Martinez, A.; Temple-Boyer, P. *Microelectron. J.* **2006**, *37*, 133–136.
(18) Maurya, D. K.; Ng, W. Y.; Mahabadi, K. A.; Liang, Y. N.; Rodríguez, I. *Biotechnol. J.* **2007**, *2*, 1381–1388.
(19) Cong, H.; Pan, T. *Adv. Funct. Mater.* **2008**, *18*, 1912–1921.

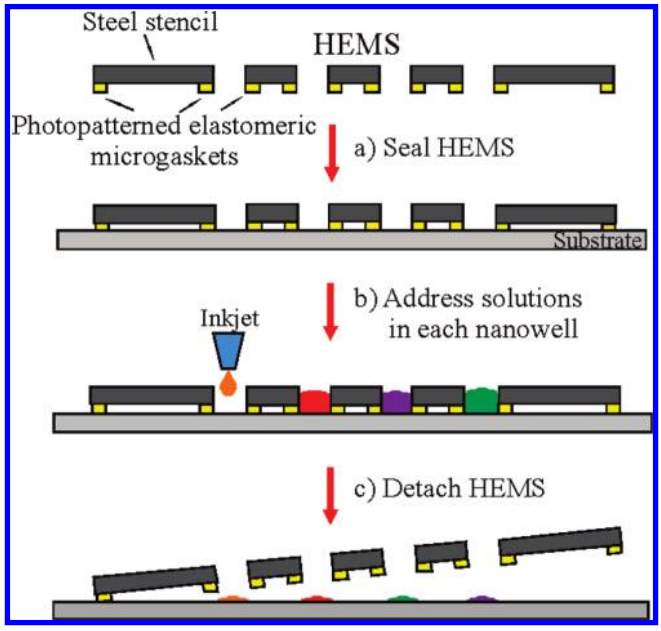

Figure 1. Schematic illustrating the use of reversibly sealable HEMS to form addressable nanowell arrays on a surface. The HEMS comprises two layers, a 50 μm thick steel stencil (dark gray) and elastomeric microgaskets (yellow) patterned around each opening. (a) The HEMS is brought into contact with a flat substrate and the microgaskets form a seal with the substrate resulting in an array of nanowells. (b) An inkjet microarrayer is used to deliver distinct solutions to each nanowell. (c) The HEMS can be detached from the surface during or at the end of the experiment.

into a positive resist, albeit with a lateral resolution limited to hundreds of micrometers.[20] None of the photosensitive silicone elastomers were suitable for our application; therefore, we evaluated five alternatives.

The specifications for our particular application are (i) softness (Shore A 50 or lower), (ii) availability of a solvent for thinning which is needed for spin-coating, (iii) homogeneous thin film formation, (iv) resolution better than 20 μm, (v) insensitivity to oxygen, (vi) complete development, and (vii) good adhesion to steel. A series of photocurable elastomers commonly used for encapsulation of electronic components such as wire bonds were tested against the above requirements (Table 1). Dymax-103, an acrylate based polymer, was the only one that could be used to reliably pattern microgaskets on steel stencils. The adhesion between photopatterned elastomers and steel represented a considerable challenge because during development the elastomers are bathed in a solvent that swells them considerably, leading to strain and detachment from the surface. We found that by functionalizing the steel with 3-(trimethoxysilyl)propyl methacrylate (TMSMA),[21] the adhesion was markedly improved and allowed production of large, defect free arrays of rings (Figure S-5 in the Supporting Information).

The patterning of microgaskets on steel stencils faced an additional challenge because of the openings present in the steel stencil. Upon spin-coating of Dymax-103, an inhomogeneous layer was formed around these openings, which in turn resulted in many defective microgaskets. To remedy this problem, we introduced an intermediate substrate that was spin-coated with the photocurable elastomer and then pressed against the steel stencil (Figure 2). As an intermediate substrate, a coverslip was used because it is thin and transparent, which are two requirements as the coverslip is placed between the photosensitive layer and the photomask. Although the 170 μm gap formed between photomask and the photosensitive layer leads to a loss in resolution, it remained sufficient for this particular application as illustrated by the HEMS shown in Figure 2. The photopatterned microgaskets were approximately 10 μm thick and 44 ± 4 μm wide, which is 17% wider than the feature size on the mask (35 μm). Part of the enlargement may also be due to the limited resolution of Dymax-103. On the basis of our experiments, we could resolve features separated by 9 ± 4 μm when a 10 μm thick Dymax-103 layer was used, which suggests that 1:1 is close to the maximal aspect ratio that can be achieved with this photocurable elastomer and which, therefore, likely contributes to the enlargement at the edge.

The alignment between the steel stencil openings and the photomask with the microgasket designs was achieved easily by the use of alignment marks featured both on the photomask and the stencil (Figure S-2 in the Supporting Information). The intermediate substrate also resolves the issue of contamination of the photomask following a contact with the photoelastomer. By physically isolating the photomask from the substrate during the alignment with the stencil, we could use the photomask repeatedly without cleaning it.

Although the HEMSs used in our experiments feature large areas without openings, the microgaskets cover the entire surface (Figure 2). This design brings about two advantages. The first one is that a single photomask can be used with stencils containing different configurations of subarrays as long as the opening-to-opening distance is conserved. The second one is that the multiplicity of microgaskets leads to a stronger and homogeneously distributed adhesion between the stencil and the substrate because of the larger number of contact points.

We noticed that the fabrication yield was close to 100% for microgaskets patterned around openings whereas the ones located on the areas between subarrays had many defects (Figure S-6 in the Supporting Information). We found that air bubbles could be trapped during the fabrication process when the coverslip is pressed against the steel stencil and led to defects in the areas without openings. In the areas with openings, trapped air can easily escape and defects are, thus, avoided. The HEMSs are robust and resilient, can be cleaned with detergents, and can be sterilized under UV light, oxygen peroxide based solutions, and ethanol, and can be heated to at least 100 °C.

As expected by virtue of the softness of Dymax-103 (Shore A 25), the HEMSs can be sealed, removed, and resealed multiple times on any smooth surface. We tested whether the sealing was liquid-tight on both hydrophobic and hydrophilic surfaces (Figure S-7 in the Supporting Information). The filled nanowells were kept in a humidified environment to prevent evaporation, and liquid was efficiently confined for at least 12 h on hydrophobic surfaces, such as an epoxy-coated microscope slide or native polystyrene Petri dish, and on hydrophilic surfaces such as plasma treated polystyrene or a polylysine coated glass slide. The stencils have

(20) Bhagat, A. A.; Jothimuthu, P.; Papautsky, I. *Lab Chip* **2007**, *7*, 1192–1197.
(21) Moeller, H.-C.; Mian, M. K.; Shrivastava, S.; Chung, B. G.; Khademhosseini, A. *Biomaterials* **2008**, *29*, 752–763.

Table 1. UV Photocurable Elastomers Evaluated

photocurable elastomer (Shore[a], monomer)	solvent solubility for thin-film deposition	thin-film deposition	UV exposure time (356 nm, 11.5 mW/cm^2)	development	adhesion to native steel	adhesion to treated steel with TMSMA[b]
Dymax 107 Shore A 40 urethane acrylate	failed to identify suitable solvent					
Dymax 105 Shore A 15 polybutadiene acrylate	2:1 (toluene) 2:1 (MEK) 2:1 (DCM)	nonhomogeneous thin layer (presence of aggregates)				
Semicosil 964 UV Shore A 30 RTV-1 amine cure silicone	2:1 (toluene) 2:1 (xylene)	homogeneous thin layer	no cross-linking observed			
Semicosil 936 Shore A 30 RTV-1 amine cure silicone	2:1 (toluene) 2:1 (xylene)	homogeneous thin layer	100 s	nonexposed areas did not dissolve		
Dymax 103 Shore A 25 polybutadiene acrylate	2:1 (toluene) 2:1 (MEK) 2:1 (xylene) 2:1 (chloroform)	homogeneous thin layer	30 s (>30 s poor resolution)	toluene, chloroform, xylene (10 s)	failure of many gaskets	good

[a] Shore or hardness. PDMS (Sylgard 184) has Shore A 50. [b] TMSMA: 3-(trimethoxysilyl)propyl methacrylate.

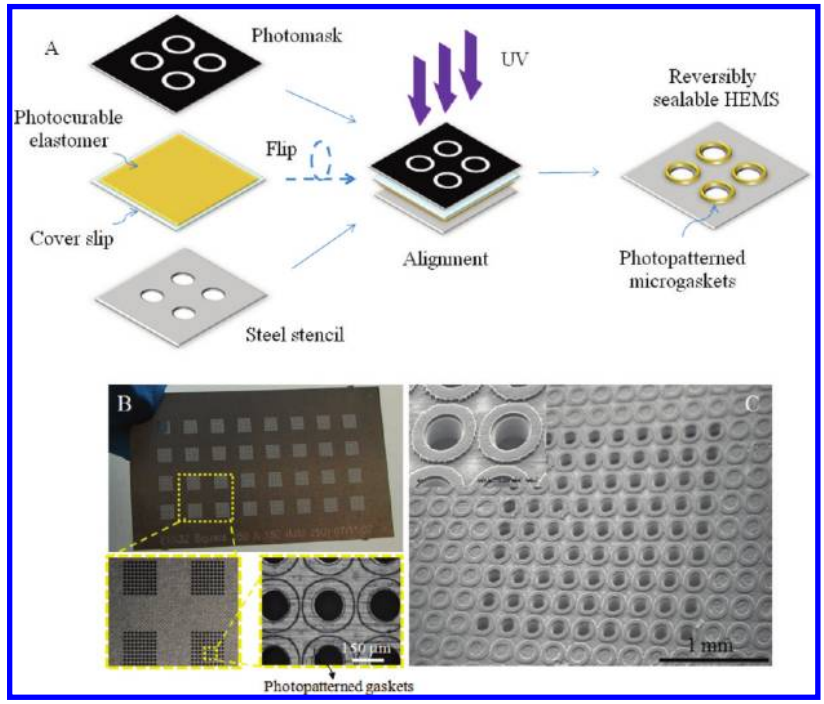

Figure 2. Schematic illustrating the fabrication process and images of HEMS. (A) A coverslip is spin-coated with a thin layer of photocurable elastomer and sandwiched between a steel stencil and the photomask. The photomask is aligned with the stencil, and then the photocurable elastomer is exposed to UV. Finally, the coverslip is peeled off, and the unexposed photocurable elastomer is developed yielding a HEMS with the photopatterned microgaskets surrounding each opening. (B) Optical images showing the stencil from the back with insets of the microgaskets. (C) SEM micrograph of the patterned microgaskets.

been used up to 10 times on different surfaces without losing their sealing properties.

Defects or dirt can nevertheless lead to leakage of fluids, and the microgasket design represents a robust approach that minimizes the consequences of a leakage. Instead of microgaskets, it might have been easier to coat the entire steel with the elastomer and form openings only where there was an opening in the steel stencil, which would have provided a much larger sealing area between the HEMS and the substrate. However, in this configuration, when liquids starts to creep between the elastomer and the substrate, it can spread across the entire surface leading to catastrophic sealing failure and mixing of fluids from different gaskets. Catastrophic failures are particularly difficult to prevent, and sometimes to identify, when hydrophilic substrates are used. In the design shown here with individual gaskets, the failure is more likely to remain confined to a single gasket, since it is disconnected from the others. Indeed, when failure occurs, the liquid tends to spread along the elastomer ring but does generally

Figure 3. Integration of HEMS with commonly used and custom-made gaskets for incubating different subarrays of the HEMS with each a different sample. (A) HEMS clamped and sealed using common 16-well gaskets each separated by 9 mm. Only 8 wells overlap with the HEMS. (B) Custom designed, laser cut gasket where wells separated by 4.5 mm are sealed directly atop of the HEMS forming one well atop of each subarray. Scale bar 2 mm.

not spread beyond the rim of the gasket which acts as a capillary valve.[16]

Several HEMS could be processed simultaneously which helped minimize fabrication time. The patterned steel stencils were obtained from commercial vendors at a cost of ~$10 per stencil. Considering that HEMS are reusable and that the costs of the individual stencils could be further reduced when ordered in large volumes, they represent a cost-effective approach to making nanowell arrays.

In an effort to make nanowell arrays compatible with commercial and custom-made multiwell gaskets (Figure 3), they were designed as 32 subarrays of 81 nanowells with a 4.5 mm pitch between two subarrays, which corresponds to the spacing of a 384 well plate and conforms to the ANSI standard used throughout the industry. The use of multiwell gaskets allows the incubation of each subarray with a different solution, which is useful for testing different samples or for producing dilution series for calibration purposes. These wells can be addressed manually or using standard pipetting robots.

Individual addressing of the nanowells represents a challenge because the nanowells are so small (~140 μm wide) and so close together that they cannot be addressed either by hand or using standard pipetting robots. We, therefore, used an inkjet spotter with a video image recognition system to address the wells individually. Compared to conventional microarrays, where all spots are aligned relative to one another, absolute alignment is required to target each of the wells. The image recognition system relaxes the requirements for absolute alignment of the HEMS because the corners of an array or a subarray can be identified on-the-fly using an image recognition feature, and used as a reference to calculate the relative XY positions of the other nanowells on the array (ac10033d_si_002.avi in the Supporting Information). Steel is highly reflective, and the contrast between the nanowells (dark) and the steel stencil (bright) greatly facilitates the image recognition process.

Despite accurate alignment, we found that many droplets were often spotted outside the wells in an apparently random fashion (Figure S-8 in the Supporting Information). One source for stray spotting is contamination of the pipet tip which typically leads to a systematic deflection of the spots; however, this could not account for the random distribution. We found that after contacting the sealed HEMS with an antistatic gun, the spots could be reliably delivered to individual nanowells. Figure 4 shows a protein microarray with green and red fluorescently labeled proteins (goat immunoglobulin labeled with AF488 and streptavidin labeled with AF548) that were patterned on an epoxy coated slide using the nanowells.

One of the well-known issues with flat arrays is the so-called "ring effect" that leads to an accumulation of material at the edges of the spots. Despite a different geometry, the same pattern is reproduced when the nanowells were used, as can be seen with the red spots in Figure 4. The mechanism by which more material accumulates at the edges is presumably different since the droplets are pinned at the steel wall of the nanowells and form a concave meniscus within the nanowells, as opposed to a convex droplet shape on a flat surface.[22] Another common issue with protein microarrays are "comets" formed around the spots as a consequence of washing solution displacing the protein droplet along the surface leaving a trail of adsorbed proteins in its wake. Although this effect can be minimized by optimizing the washing process, the use of HEMS eliminates the comets altogether because the stencil protects the space between spots. In addition, the protein microarrays obtained are perfectly aligned despite minor spotting inaccuracies of the inkjet.

PDMS stencils have been used extensively to study how patterning cells in isolated groups affect cell−cell interaction and cell development. Cocultures obtained after backfilling patterned arrays of cells with another type of cell have been used for tissue engineering.[11,23,24] HEMSs ensure that patterned cells will be perfectly aligned which in turn facilitates the automatic acquisition of images with microscopes equipped with motorized XY stages. We used HEMSs to pattern C2C12 myoblast cells on polystyrene Petri dishes. Once the cell adhered and spread on the polystyrene, the stencil was removed yielding an array of cells (Figure 4). No difference was apparent between patterned and nonpatterned cells, supporting the notion that HEMSs are biocompatible. The microgaskets of the HEMS do not leave any observable residue or footprint on the surface, and the cells growing on the contact areas did not exhibit any difference with cells grown on a pristine surface. Similar results were obtained using HEK 293T human epithelial kidney cells (results not shown). As described above, HEMSs may be used in combination with multiwell gaskets, allowing the patterning of distinct cell types on the same surface by hand.

Reverse transfection microarrays involve culturing cells over DNA constructs microarrayed on a substrate and monitoring expression within cells that adhere over the distinct microarray spots.[25,26] Here, we show that HEMS can be used to confine the cells physically within a nanowell which eliminates the risk of

(22) Hjelt, K. T.; Lubking, G. W.; Vellekoop, M. J.; Vliet, L. J. v.; Doel, L. R. v. d.; Greiner, A.; Korvink, J. G. *Sens. Update* **2000**, *8*, 39–70.
(23) Jinno, S.; Moeller, H.-C.; Chen, C.-L.; Rajalingam, B.; Bong, G. C.; Dokmeci, M. R.; Khademhosseini, A. *J. Biomed. Mater. Res., Part A* **2008**, *86*, 278–288.
(24) Khademhosseini, A.; Ferreira, L.; Blumling, J., III; Yeh, J.; Karp, J. M.; Fukuda, J.; Langer, R. *Biomaterials* **2006**, *27*, 5968–5977.
(25) Ziauddin, J.; Sabatini, D. M. *Nature* **2001**, *411*, 107–110.
(26) Wu, R. Z.; Bailey, S. N.; Sabatini, D. M. *Trends Cell Biol.* **2002**, *12*, 485–488.

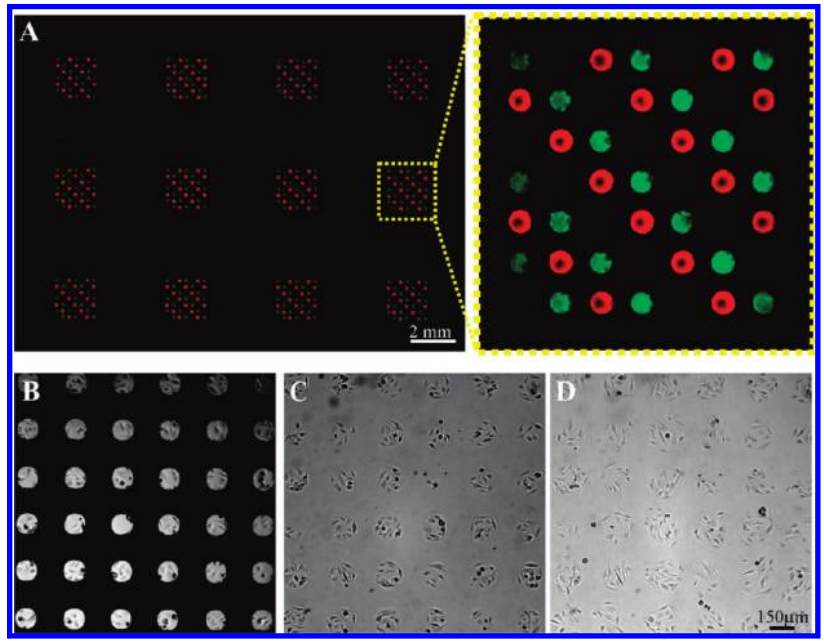

Figure 4. Patterning proteins and cells as microarrays using HEMS. (A) Scanning fluorescence image and inset showing an array of goat immunoglobulin labeled with AF488 green fluorescent dye (green channel) and streptavidin labeled with AF548 red fluorescent (red channel). The fluorescently labeled protein patterns were formed on an epoxy slide formed by dispensing two different solutions on the arrays of nanowells. (B) Differential interference contrast micrograph of C2C12 myoblasts that were seeded over the HEMS and adhered within the nanowells on the surface of a polystyrene Petri dish. (C) The cells immediately after removal of the HEMS and (D) 4 h later showing that the cells spread beyond the original patterns.

cross-contamination between different spots. Reporter plasmid constructs encoding EGFP (green fluorescent protein) and ECFP (cyan fluorescent protein) were spotted into a series of distinct nanowells. HEK 293T kidney cells were seeded as described above, and upon reverse transfection, expressed either EGFP or ECFP, while remaining confined within their respective nanowell (Figure 5). We performed time lapse imaging of the transfection of cells in 3 channels (EGFP, ECFP, and brightfield) over a period of 24 h (ac100335d_si_003.avi in the Supporting Information) illustrating the use of HEMS for live imaging. The collection of images was initiated 24 h after seeding the cells, which is the time required for reaching the steady state for the fluorescent signals reporting the cell transfection. During this period, the cell has to attach to the bottom of the wells and the plasmid has to enter the cells and reach the nucleus.

Conventional reverse transfection microarray assays are performed in our lab by printing 6.7 nL of DNA solution per 400 μm spot, resulting in approximately ~100 transfected HEK 293T cells out of a total of 300 per spot corresponding to ~30% yield. Here, by printing 1.2 nL, into a 140 μm well, approximately 5 to 6 cells, mostly on the periphery, out of a total of ~30 cells were transfected (20% yield). The efficiency is slightly lower than in a conventional setup, and we attribute it to the inhomogeneous distribution of the DNA constructs and their accumulation at the periphery of the wells caused by the fast drying of the solutions at the center of the nanowells. For routine application of HEMS to cell transfection, the size of the wells will need to be increased to accommodate a statistically significant number of cells, and the concentration of DNA constructs and the drying of liquid (dependent on the contact angle with sidewall and well bottom) would need to be optimized.

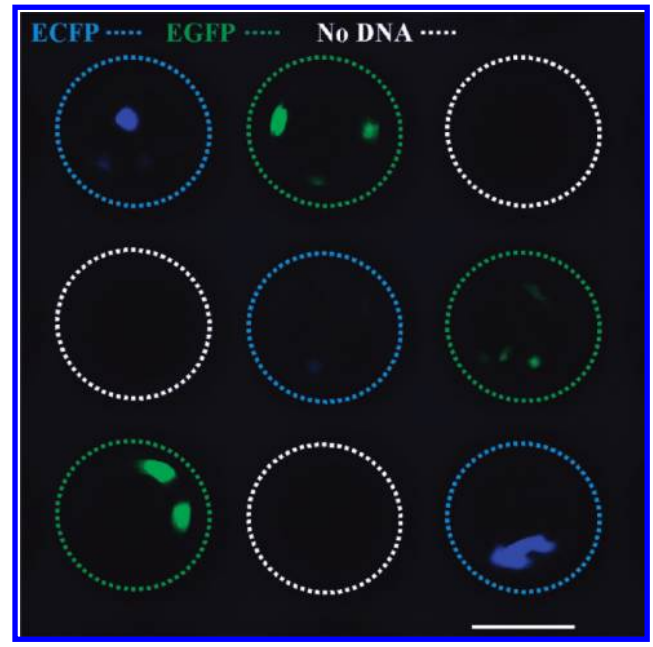

Figure 5. Reverse transfected HEK 293T kidney cells on nanowells. Nanowells were addressed with three droplets of reporter plasmid encoding cyan fluorescent protein (ECFP, indicated with cyan circle), green fluorescent protein (EGFP, indicated with green circle), or no DNA (white circle). Cells were incubated in the wells, and fluorescence images were taken after 24 h. A time lapse video using composite DIC and fluorescence imaging is shown in ac100335d_si_003.avi in the Supporting Information. Scale bar 150 μm.

CONCLUSIONS

We described the microfabrication of HEMS and discussed the challenges associated with photopatterning elastomeric microgaskets. We constructed HEMS based nanowell arrays with 2592 wells arranged in 32 subarrays with each having 81 wells

spaced 250 μm apart and with a capacity of ~1 nL and demonstrated their use on hydrophilic and hydrophobic surfaces.

HEMSs were combined with microgaskets to allow for manual addressing of subarrays, while individual addressing of nanowells by a robotic an inkjet printer was made possible by the favorable mechanical properties of and high optical contrast of the steel stencils. HEMSs were used to make protein arrays by first spotting distinct protein solutions into nanowells followed by removal of the HEMS from the substrate. Finally, we used time-lapse imaging to visualize mammalian cells reverse-transfected with expression vectors encoding different fluorescent proteins.

The key characteristics of HEMSs are that they can be reversibly sealed on flat surfaces and form an array of regularly arranged nanowells that can be addressed with automatic liquid handling systems. A HEMS used in combination with glass substrates greatly facilitates imaging, which is particularly useful for cell studies. Transfection microarrays have traditionally been limited to adherent cells lines with low motility, since cell migration can lead to mixing of cells from different spots. HEMSs could, therefore, be potentially useful in the transfection and visualization of motile and nonadherent cells, since the cells will be physically confined by the 3D topography of the nanowells.

ACKNOWLEDGMENT

We thank the Canadian Institutes for Health Research (CIHR), Genome Canada, Genome Quebec, and the Canada Foundation for Innovation (CFI) for financial support. We would like to acknowledge the assistance of the McGill Nanotools Microfab Laboratory (funded by CFI, NSERC, and VRQ), Rob Sladek for helpful discussions, and Benjamin Robledo and Roozbeh Safavieh for their help on the microfabrication process. M.P.-R. acknowledges financial support from Spanish Ministry of Science through a postdoctoral fellowship, and D.J. acknowledges support from a Canada Research Chair.

SUPPORTING INFORMATION AVAILABLE

Additional information as noted in text. This material is available free of charge via the Internet at http://pubs.acs.org.

Received for review February 5, 2010. Accepted March 24, 2010.

AC100335D